1. Grzegorz KŁOSOWSKI[1], 2. Michał STYŁA[2], 3. Dominik GNAŚ[2], 4. Wiktoria ZAWADZKA[4], 5. Przemysław ADAMKIEWICZ [2,3]

Lublin University of Technology (1),
Information Technology Research & Development Center (CBRTI Sp. z o.o.), Rzeszów (2), WSEI University (3),
ORCID: 1. 0000-0001-7927-3674, 2. 0000-0002-1141-0887; 3. 0000-0002-8169-9700; 4. 0009-0008-8139-1555; 5. 0000-0003-3425-9566

doi:10.15199/48.2025.01.33

The concept of low-energy radio transceivers and residual networks for advanced radio tomography in building localization

***Abstract**. This study aims to advance the field of Radio Tomography Imaging (RTI), focusing on device-free methods for human localization within confined environments. Utilizing deep residual networks, the research transforms Wi-Fi Received Signal Strength Indicator (RSSI) data into tomographic images, thereby contributing algorithmic advancements to RTI. Such a device-free approach circumvents the need for monitored individuals to carry electronic devices, ensuring privacy protection through inherent anonymization. Alongside, this work presents the development of optimized, energy-efficient hardware specifically designed for RTI applications. Considering real-world constraints, the hardware architecture reconciles performance, energy efficiency, and device compatibility. The study adopts a holistic framework that integrates both the algorithmic and hardware aspects of RTI, providing a comprehensive solution for real-world deployments. By examining Wi-Fi-based RTI through both an algorithmic lens, using deep residual networks, and a hardware-centric perspective, this research paves the way for scalable, efficient, and privacy-preserving localization systems. The objective is to present a balanced, optimized approach that contributes to developing state-of-the-art RTI methods and implementations.*

***Streszczenie.** Celem niniejszych badań jest rozwój dziedziny obrazowania radiotomograficznego (RTI), które koncentrują się na metodach lokalizacji człowieka w zamkniętych środowiskach, niewymagających stosowania dodatkowych urządzeń. Wykorzystując głębokie sieci rezydualne, w badaniach przeprowadzono transformację danych wskaźnika siły sygnału odebranego Wi-Fi (RSSI) na obrazy tomograficzne, przyczyniając się w ten sposób do udoskonalenia algorytmów w dziedzinie RTI. Takie podejście, niewymagające użycia urządzeń, pozwala uniknąć konieczności noszenia przez monitorowane osoby urządzeń elektronicznych, zapewniając w ten sposób ochronę prywatności poprzez anonimizację. W pracy przedstawiono także rozwój zoptymalizowanego, energooszczędnego sprzętu zaprojektowanego specjalnie do zastosowań RTI. Architektura sprzętowa łączy wydajność, efektywność energetyczną i kompatybilność urządzeń, biorąc pod uwagę ograniczenia świata rzeczywistego. W badaniu przyjęto holistyczne ramy, które integrują zarówno algorytmiczne, jak i sprzętowe aspekty RTI, zapewniając kompleksowe rozwiązanie ukierunkowane na wdrożenia w świecie realnym. Badając RTI oparte na Wi-Fi zarówno przez pryzmat algorytmu wykorzystującego głębokie sieci resztkowe, jak i perspektywę skupioną na sprzęcie, przedstawione badania torują drogę dla skalowalnych, wydajnych i chroniących prywatność systemów lokalizacji. Celem ogólnym jest przedstawienie koncepcji zrównoważonego, zoptymalizowanego podejścia, które przyczynia się do rozwoju najnowocześniejszych metod i wdrożeń RTI (**Koncepcja niskoenergetycznych radiotelefonów i sieci resztkowych dla zaawansowanej radiotomografii w lokalizacji wewnątrzbudynkowej**).*

Keywords: electrical tomography; machine learning; industrial tomography; transmission radio tomography
Słowa kluczowe: tomografia elektryczna; uczenie maszynowe; tomografia przemysłowa; radiowa tomografia transmisyjna

Introduction

Radio tomography imaging (RTI) is a critical technique for determining human presence within a confined area [1,2]. RTI methods can be broadly classified into device-based and device-free categories. This research emphasizes the device-free paradigm of RTI, which not only obviates the need for monitored individuals to carry additional electronic devices but also offers an inherent layer of privacy protection [3]. RTI inherently anonymizes monitored individuals by not revealing distinct faces or other identifying features; it simply localizes their positions within the monitored area. Coinciding with the ubiquity of Wi-Fi (IEEE 802.11) networks in modern environments, this study also explores the advancements in Wi-Fi-based localization techniques by analyzing Received Signal Strength Indicator (RSSI) data [4]. We employ deep residual networks to transform these RSSI measurements into meaningful tomograms. The radio-sensing apparatus predominantly employs commercial radiotelecommunication paradigms that adhere scrupulously to guidelines promulgated by the Institute of Electrical and Electronics Engineers (IEEE) [5]. Protocols of notable mention include Bluetooth Low Energy (LE) from the contemporary generation, ZigBee, and Wireless Fidelity (Wi-Fi), all functioning within the ubiquitously adopted 2.4 GHz Industrial, Scientific and Medical (ISM) frequency band. Such protocol adherence assures elevated congruity with diverse apparatuses within the integrated system, irrespective of manufacturing provenance or user-end devices [6,7].

Hardware

In the architecture of these devices, the pivotal component employed was a microcontroller semiconductor, specifically of the WSoC (Wireless System on a Chip) variety [8]. Auxiliary segments, contingent upon the particular system configuration, further augmented this. The predominant output frameworks incorporated were the NS nRF52832 and SL EM357 integrated circuits. Succeeding iterations of the probe are visually delineated in Fig. 1.

The NS nRF52832 is a Bluetooth Low Energy (BLE) System-on-Chip (SoC) that operates on a 32-bit ARM Cortex-M4F CPU. Designed for low-power wireless applications, this IC is equipped with 512kB of flash memory and 64kB of RAM. Its I/O capabilities include support for Serial Peripheral Interface (SPI), Universal Asynchronous Receiver-Transmitter (UART), and Inter-Integrated Circuit (I2C), thereby offering versatile connectivity options. Furthermore, the chip incorporates Advanced Encryption Standard (AES) hardware encryption to ensure data integrity and security. It complies with Bluetooth 5.0 specifications, ensuring broad interoperability with many wireless devices.

Conversely, the SL EM357 is a Zigbee-compliant IC tailored for wireless sensor networks and Internet of Things (IoT) applications. Built on the ARM Cortex-M3 processor, the EM357 is optimized for low-latency data transmission and is scalable across various network configurations. Its energy-efficient architecture makes it suitable for long-term deployments in sensor networks. Security features include AES-128 encryption and decryption capabilities. The IC supports multiple network topologies, such as point-to-point,

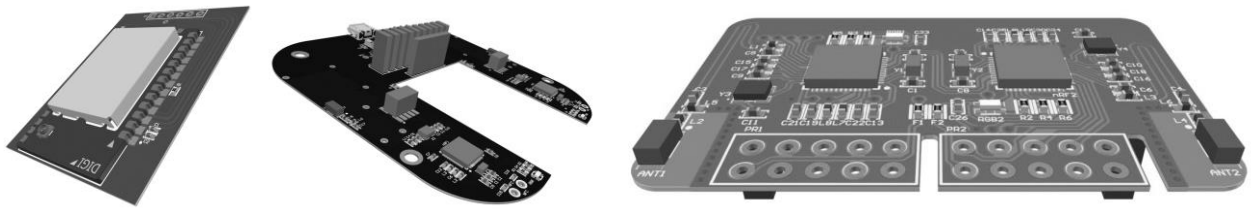

(a) (b) (c)

Fig.1. Subsequent revisions of RTI probes: (a) – ZigBee communication expander, (b) – prototype multirole probe with space for ZigBee communication module expander, (c) – miniaturized BLE probe

point-to-multipoint, and mesh networks, providing flexibility in system design.

While the NS nRF52832 and SL EM357 are engineered for low-power, wireless applications, they diverge significantly in their communication protocols and target use cases. Due to its BLE capabilities, the nRF52832 is predominantly utilized in consumer electronics, including wearables and smart home devices. In contrast, due to its Zigbee compliance, the SL EM357 is geared towards industrial applications, particularly in automation systems and sensor networks.

Integrating the NS nRF52832 or the SL EM357 into output frameworks is contingent upon the specific operational requirements, such as data throughput, power consumption, and network topology. Therefore, a nuanced understanding of the technical specifications and capabilities of each IC is imperative for achieving optimal system performance.

The inherent and default LDO (Low-Dropout) stabilizer was supplanted with an extrinsic charge pump and a DC/DC converter mechanism to attain a nadir in electrical power consumption. Irrespective of the hardware schema employed, this maneuver culminated in a zenith current drain of 32 milliamperes and an arithmetic mean of 460 microamperes, metrics attributable to each RTI (Radio Tomography Imaging) probe. It should be noted that these quantifiable parameters could exhibit minor oscillations, contingent on the probe version and overarching system model.

For the bidirectional radio frequency pathway, a ceramic resonator possessing omnidirectional propensities was chosen for BLE (Bluetooth Low Energy) configurations, while a planar antenna was selected for the u.FL interfaces compatible with ZigBee. The strategic positioning of the planar antenna, facilitated by a shielded conductive medium, diminished the systems' adverse reciprocal interactivity. Both RF (Radio Frequency) conduit systems incorporated congruent circuits, filtrations, and rigorous control of impedance attributes.

Invariable across diverse configurations, dual radio modules could be affixed to each probe, capable of sustaining either unidirectional or bidirectional data transmission. In the context of the isolated archetype of the probe, a singular BLE transmissive and receptive unit is integrated. The sequential model predicates its operation on a BLE transmission unit coupled with a ZigBee transceiver. Conversely, the mesh network topology uniquely accommodates a monolithic radio stratum, contingent nonetheless on the connectivity topology between the radio tomographic apparatus and the remainder of the network architecture—that is, the presence or absence of an intermediary node within the ensuing mesh infrastructure and the specific Bluetooth devices serving as conduits for the RSSI (Received Signal Strength Indicator) matrix to the computational cluster. The terminal radio probes within any specified category (such as the ultimate probe in Figure 1) remain confined in dimensions to that of a matchbox.

Nonetheless, these devices are not amenable to battery-powered schemes due to their protracted and intensive operational periods. They necessitate unswerving access to either a 3.3 V or a 5 V electrical grid. This requirement predicates the prerequisite for meticulous preparation of the edifice's electrical infrastructure.

The Method

In device-free human localization, an entity's identification and positioning fundamentally shift the radio frequency signals' emanation patterns. This alteration is most conspicuous within the 2.4 GHz frequency spectrum, endorsed by multiple IEEE standards such as 802.15.4, 802.11b, and 802.11g [9]. Principal methodologies formulated for unaided foreman localization encompass Triangulation, Trilateration, Hyperbolic Lateralization, among other locational determination techniques.

Commonly employed metrics for constructing device-independent tracking and localization systems include Time of Arrival (TOA), Time Difference of Arrival (TDOA), Angle of Arrival (AOA), and Direction of Arrival (DOA), frequently denoted as the Received Signal Strength Indicator (RSSI). Underpinning these mechanisms are the Received Signal Strength (RSS) indices of the wireless network, constituting the crux of radio tomographic imaging [10]. If one conceives link shadow loss due to attenuation induced by environmental elements and intervening matter between the transmitter and receiver, link shadowing metrics (RSSI values) can be harnessed to identify such matter. Utilizing this inversional viewpoint to observe substantial shadowing losses across intersecting links allows the attenuating object's locale triangulation to present a quintessential tomographic inverse problem defined by a dearth of data points relative to pixel count in the reconstructed portrayal [11-14].

The paper's seminal contribution lies in leveraging an exceptionally deep residual neural network architecture, specifically a ResNet comprising 104 layers and 1.6 million trainable parameters. Residual Neural Networks, or ResNets, have found ubiquitous applications across diverse computer vision pursuits, from object categorization to image segmentation. Fundamental to ResNets are architectural nuances such as shortcut conduits, residual modules, identity mappings, and profound architectural depth. These shortcut or 'skip' conduits facilitate the transference of information across multiple layers, ameliorating the vanishing gradient conundrum inherent in profoundly deep networks. The elemental structural unit of a ResNet is the residual block, consisting of a sequence of convolutional layers accompanied by batch normalization and ReLU activation functions. An additive shortcut connection is merged with the residual block's output. Identity mappings within ResNets allow for an uninhibited data flow from input to output, preserving the integrity of original data. The depth of the

architecture affords superior precision in intricate tasks such as image reconstitution.

Moreover, ResNets can undergo preliminary training on expansive data conglomerates like ImageNet, augmenting their efficacy across disparate computational tasks. Predominantly, the virtuosity of ResNets lies in their aptitude for training substantially deep neural networks sans the detriment of vanishing gradient issues, culminating in marked augmentations in performance metrics across various computer vision challenges.

Fig. 2 delineates the nine-block residual network architecture employed in this investigative endeavor.

Results

In order to assess the quality of the neural network, a

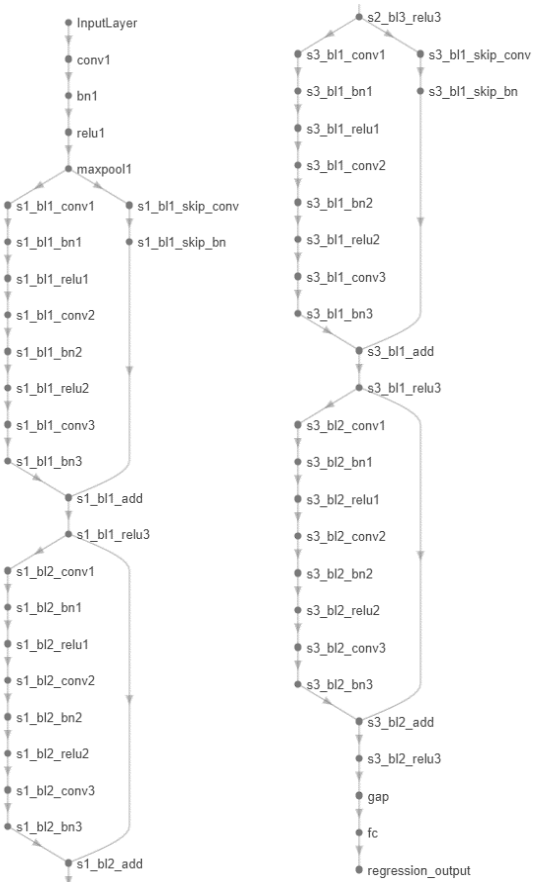

(a) **(b)**

Fig. 2. The nine-block residual network architecture: (a) – the primary blocks, (b) – the terminal blocks

number of test reconstructions were made, which enabled the perceptual comparison of tomograms with reference images. In order to avoid subjectivity during the assessment, quantitative measures were also used. The inaugural metric for assessment utilized was the Mean Square Error (MSE), delineated by the equation (1):

$$\mathrm{MSE} = \sum_{i=1}^{n} \frac{(y_i - y_i^*)^2}{n} \tag{1}$$

In this mathematical representation, y_i embodies the prototypical image replete with *n* volumetric pixels, while y_i^* symbolizes the reassembled image. The total pixel count for the image, denoted as *n*, is precisely 5329.

Subsequent to the MSE, the study incorporated the Peak Signal-To-Noise Ratio (PSNR) which is defined as [15-18]:

$$\mathrm{PSNR} = 10 \cdot \log_{10}(R^2/MSE) \tag{2}$$

For this investigative scrutiny, *R* was selected as unity. It characterizes the uppermost permissible variance in pixel values for constructing the preliminary image. PSNR is a robust gauge for the emanated signal in juxtaposition with ambient noise in the reconstituted image tableau.

However, another evaluative metric employed was the Structural Similarity Index Measure (SSIM), a composite measure fusing disparate facets such as luminosity, local structural motifs, and contrast. The characteristic termed 'structural integrity' encloses the luminance configurations of the Finite Element Mesh (FEM) constituents, considering adjacent volumetric pixels. Mathematically, SSIM is defined by:

$$\mathrm{SSIM} = \frac{(2\mu_{y^*}\mu_y + \mathrm{C}_1)(2\sigma_{y^*y} + \mathrm{C}_2)}{(\mu_{y^*}^2 + \mu_y^2 + \mathrm{C}_1)(\sigma_{y^*}^2 + \sigma_y^2 + \mathrm{C}_2)} \tag{3}$$

Herein, $\mu_{y^*}, \mu_y, \sigma_{y^*}, \sigma_y$ and $*\sigma_{y^*y}$ denote local averages, standard deviations, and cross-covariance of the images y^* and y. $C_1 = (0.01 \cdot L)^2$ and $C_2 = (0.03 \cdot L)^2$. If the pixel values are within the range (0,1), as in this case, *L*=1.

Concluding the panoply of evaluative metrics is the Image Correlation Coefficient (ICC), captured by:

$$\mathrm{ICC} = \frac{\sum_{i=1}^{n}(y_i - \bar{y})\left(y^*{}_i - \overline{y^*}\right)}{\sqrt{\sum_{i=1}^{n}(y_i - \bar{y})^2 \sum_{i=1}^{n}\left(y^*{}_i - \overline{y^*}\right)^2}} \tag{4}$$

Where $\overline{y^*}$ and $\bar{y}$ are, respectively, the arithmetic means of pixel values for the reconstituted and benchmark images.

Fig. 3 compares pattern images with RTI reconstructions obtained using ResNet. The obtained reconstructions are of high quality. The colored circles in the tomograms result from image filtering based on the pixel value segmentation method.

Table 1 presents a comparison of the reconstruction quality coefficients. The cases in Table 1 correspond to the images in Figure 3. Low MSE error values and high values of other indicators prove the high efficiency of the tested neural network.

Table 1. Reconstruction quality assessment indicators

#	MSE	PSNR	SSIM	ICC
1	0.0042	23.7428	0.5314	0.8904
2	0.0060	22.1859	0.4066	0.8280
3	0.0050	23.0476	0.4577	0.8496

Conclusions

The study presents an analysis of the effectiveness of using a neural residual network to solve the inverse problem in radio tomography for tracking the movement of people in rooms. The study innovatively used a residual neural network (ResNet) of 104 layers and 1.6 million trainable parameters to enable human location. This complex architecture overcame the challenges inherent in deep network training, particularly the vanishing gradient problem, thus offering greater accuracy for complex tasks such as tomographic reconstruction.

In addition, the concept of low-power wireless integrated circuits (ICs), namely NS nRF52832 and SL EM357, was presented in the field of device-less human location. These ICs were intended for a wide variety of applications. While the former found its way into consumer electronics due to Bluetooth Low Energy (BLE) capabilities, the latter was adapted to industrial applications and the Internet of Things (IoT), attributed to Zigbee compatibility. The architecture provided scalability and energy efficiency to meet various

operational requirements across different network topologies. Particular attention has been paid to optimizing power consumption by replacing the built-in LDO regulator, achieving a zenith current draw of 32 milliamps and an average of 460 microamps.

Performance evaluation was performed using a set of quantitative metrics, including mean squared error (MSE), peak signal-to-noise ratio (PSNR), structural similarity index (SSIM) measure, and image correlation coefficient (ICC). These metrics enabled a multidimensional assessment, confirming the effectiveness of the applied methodologies in achieving precise human localization and image reconstruction.

Key technological features such as RF path selection and bi-directional data capabilities are also explained, offering insight into their impact on system performance and architecture scalability. The study, therefore, underlined the need for a detailed understanding of both hardware and algorithmic aspects to ensure optimal performance of human locating systems based on radio tomography.

The research is a significant step towards developing reliable, efficient, scalable, device-free human location systems. Future work could explore the integration of more advanced machine learning algorithms and consider alternative chips for further optimization. The search for energy-efficient designs and the applicability of the proposed system in real-life scenarios remain important areas for future research.

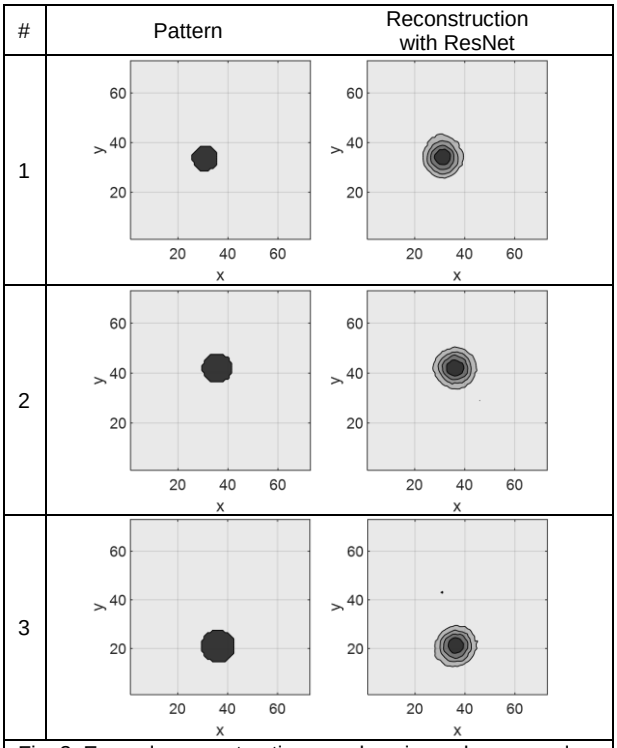

Fig. 3. Example reconstructions made using a deep neural network with ResNet architecture

***Authors**: Grzegorz Kłosowski, Ph.D. Eng., Lublin University of Technology, Nadbystrzycka 38A, Lublin, Poland, E-mail: g.klosowski@pollub.pl; Michał Styła, MSc., Centrum Badawczo Rozwojowe Technologii Informatycznych Sp. z o.o., Rzeszów, Poland, E-mail: michal.styla@cbrti.pl; Dominik Gnaś, MSc., Centrum Badawczo Rozwojowe Technologii Informatycznych Sp. z o.o., Rzeszów, Poland, E-mail: dominik.gnas@cbrti.pl; Przemysław Adamkiewicz, Ph.D., Centrum Badawczo Rozwojowe Technologii Informatycznych Sp. z o.o., Rzeszów, Poland, WSEI University, Lublin, Poland, E-mail: przemyslaw.adamkiewicz@cbrti.pl.*

REFERENCES

[1] Liu, H.; Darabi, H.; Banerjee, P.; Liu, J. Survey of Wireless Indoor Positioning Techniques and Systems. IEEE Transactions on Systems, Man and Cybernetics Part C: Applications and Reviews 37 (2007), 1067–1080.

[2] Li, X.; Huang, H.Z.; Li, Y.F.; Li, Y.F. Reliability Evaluation for VHF and UHF Bands under Different Scenarios via Propagation Loss Model. *Eksploatacja i Niezawodnosc* 21(2019), doi:10.17531/ein.2019.3.3.

[3] Pirzada, N.; Nayan, M.Y.; Hassan, F.S.M.F.; Khan, M.A. Device-Free Localization Technique for Indoor Detection and Tracking of Human Body: A Survey. *Procedia Soc Behav Sci* 129 (2014), 422–429, doi:10.1016/J.SBSPRO.2014.03.696.

[4] Gnaś, D., Adamkiewicz, P., Indoor localization system using UWB, Informatyka, Automatyka, Pomiary W Gospodarce I Ochronie Środowiska, 12 (2022), No. 1, 15-19.

[6] Wilson, J.; Patwari, N. See-through Walls: Motion Tracking Using Variance-Based Radio Tomography Networks. *IEEE Trans Mob Comput* 10 (2011), doi:10.1109/TMC.2010.175.

[7] Yigitler, H.; Jantti, R.; Kaltiokallio, O.; Patwari, N. Detector Based Radio Tomographic Imaging. *IEEE Trans Mob Comput* 17 (2017), doi:10.1109/tmc.2017.2699634.

[8] Styła, M., Adamkiewicz, P., Optimisation of commercial building management processes using user behaviour analysis systems supported by computational intelligence and RTI, Informatyka, Automatyka, Pomiary W Gospodarce I Ochronie Środowiska, 12 (2022), No 1, 28-35.

[9] Moussa, M.; Youssef, M. Smart Devices for Smart Environments: Device-Free Passive Detection in Real Environments. In Proceedings of the 7th Annual IEEE International Conference on Pervasive Computing and Communications, PerCom 2009; 2009.

[10] Wilson, J.; Patwari, N. Radio Tomographic Imaging with Wireless Networks. *IEEE Trans Mob Comput*, 9(2010), 621–632, doi:10.1109/TMC.2009.174.

[11] Patwari, N.; Wilson, J. RF Sensor Networks for Device-Free Localization: Measurements, Models, and Algorithms. In Proceedings of the Proceedings of the IEEE; 2010; Vol. 98.

[12] Gocławski, J., Sekulska-Nalewajko, J., Korzeniewska, E., Prediction of textile pilling resistance using optical coherence tomography, Scientific Reports, 12 (2022), No. 1, 18341.

[13] Gocławski, J., Korzeniewska, E., Sekulska-Nalewajko, J., Kiełbasa, P., Dróżdż, T., Method of Biomass Discrimination for Fast Assessment of Calorific Value, Energies, 15 (2022), No. 7, 2514.

[14] Kłosowski G, Rymarczyk T, Niderla K, Kulisz M, Skowron Ł, Soleimani M., Using an LSTM network to monitor industrial reactors using electrical capacitance and impedance tomography – a hybrid approach. Eksploatacja i Niezawodnosc – Maintenance and Reliability, 25 (2023), No. 1, 11.

[15] Kłosowski G., Rymarczyk T., Kania K., Świć A., Cieplak T., Maintenance of industrial reactors supported by deep learning driven ultrasound tomography, Eksploatacja i Niezawodnosc – Maintenance and Reliability; 22 (2020), No 1, 138–147.

[16] Kłosowski G., Rymarczyk T., Niderla K., Rzemieniak M., Dmowski A., Maj M., Comparison of Machine Learning Methods for Image Reconstruction Using the LSTM Classifier in Industrial Electrical Tomography, Energies 2021, 14 (2021), No. 21, 7269.

[17] Rymarczyk T., Kłosowski G., Hoła A., Sikora J., Tchórzewski P., Skowron Ł., Optimising the Use of Machine Learning Algorithms in Electrical Tomography of Building Walls: Pixel Oriented Ensemble Approach, Measurement, 188 (2022), 110581.

[18] Koulountzios P., Rymarczyk T., Soleimani M., A triple-modality ultrasound computed tomography based on full-waveform data for industrial processes, IEEE Sensors Journal, 21 (2021), No. 18, 20896-20909.

[19] Koulountzios P., Aghajanian S., Rymarczyk T., Koiranen T., Soleimani M., An Ultrasound Tomography Method for Monitoring CO2 Capture Process Involving Stirring and CaCO3 Precipitation, Sensors, 21 (2021), No. 21, 6995.